

Core effects on the energetics of solid Li at high pressure

Yansun Yao,^{1,2} John S. Tse,¹ Zhe Song,¹ and Dennis D. Klug²¹Department of Physics and Engineering Physics, University of Saskatchewan, Saskatoon, Saskatchewan, Canada S7N 5E2²Steacie Institute for Molecular Sciences, National Research Council of Canada, Ottawa, Ontario, Canada K1A 0R6

(Received 30 September 2008; revised manuscript received 22 February 2009; published 27 March 2009)

Using the recently proposed $P4_132$ structure as a test case, the accuracy of three three-electron Li pseudopotentials for plane-wave electronic structure calculations at very high pressure was examined. At high Li density ($r_s < 1.94$), it is found that carefully chosen core radii cutoffs in the construction of the pseudopotential are necessary in order to reproduce results obtained from all-electron full potential linearized augmented plane-wave method at very high pressure. This accuracy is needed to resolve small enthalpy differences between competitive polymorph phases in this pressure range. In this manner, a three-electron pseudopotential in the Troullier-Martins form was constructed. Using this pseudopotential, it is found that a previously proposed “dimer” $Cmca-8$ structure is slightly more stable than the $Cmca-24$ structure at pressure higher than 456 GPa. The $P4_132$ structure is found having higher enthalpy than both $Cmca-8$ and $Cmca-24$ structures up to at least 500 GPa.

DOI: [10.1103/PhysRevB.79.092103](https://doi.org/10.1103/PhysRevB.79.092103)

PACS number(s): 71.15.Ap, 71.20.Dg, 61.50.Ks

The effect of pressure on the electronic properties of solid Li has been a subject of many investigations. It was predicted that Li would transform to a paired “dimer” structure ($Cmca-8$) near 80 GPa.¹ A latter theoretical search revealed an orthorhombic structure ($Cmca-24$) phase that was predicted to be stable from 88 to at least 140 GPa.² Application of the genetic algorithm technique^{3–6} using a commonly used three-electron ($1s2s$) projected augmented wave (PAW) potential,⁷ available in the public released pseudopotential library (*vide infra*), confirmed that the $Cmca-24$ structure is the lowest enthalpy phase up to 300 GPa.⁸ At higher pressure up to 1 TPa, a cubic $P4_132$ structure containing sixfold coordinated Li atoms was predicted.⁸ This prediction indicates that the dimer structure would not be a stable phase up to at least 1 TPa. More recently, first-principles molecular-dynamics calculations⁹ found, at pressure lower than 100 GPa, a re-entrant behavior in the melting boundary akin to that proposed for solid hydrogen.¹⁰

It is expected that at very high density, the core ($1s$) potential would notably influence the electronic properties of Li. At ambient pressure, from experimental data the energy difference between the core and valence ($2s2p$) levels in Li is estimated to be about 50 eV.¹¹ Under compression, the valence and core bandwidth increase and this narrows the separation between $1s$ and $2s2p$ levels to ca. 40 eV. Therefore, the repulsive interaction between $1s$ and valence $2s, 2p$ orbitals is expected to be more significant. Moreover, at high pressure, the Li-Li distance can be as short as 2.46 a.u. ($P4_132$, 1 TPa) and the core orbitals of neighboring Li atoms are almost touching, therefore, careful construction of the core potential even when using a three-electron scheme is crucial in order to predict correct electronic properties. The purpose of the present study is to examine the reliability of the three-electron Li pseudopotentials, the PAW (Ref. 7) and Goedecker-Teter-Hutter (GTH) (Ref. 14) pseudopotentials, available with the Vienna *ab initio* simulation package (VASP) (Ref. 15) and ABINIT (Ref. 16) codes, respectively, by comparison to all-electron (AE) full potential linearized augmented plane-wave (FP-LAPW) methods^{17,18} using the recently proposed high-pressure Li $P4_132$ structure⁸ as the test

case. The PAW pseudopotential available in the VASP standard pseudopotential library was constructed with two s , two p , and one d channels with the d channel chosen as local. The two projectors for the same orbital angular momentum (l) were used to describe the bounded and unbounded states. The cutoff radii are 1.55 and 2.05 a.u. for the two s channels, 2.05 a.u. for both p channels, and 1.55 a.u. for the d channel. An energy cutoff of 400 eV yielded excellent convergence of total energy for this potential.⁸ Furthermore, a hard three-electron pseudopotential in the Troullier-Martins (TM) (Ref. 19) form suitable for the QUANTUM-ESPRESSO (QE) package²⁰ is constructed and validated. The TM pseudopotential was generated with $1s$, $2s$, and $2p$ channels and the $2p$ channel was treated as local. The valence wave functions for the three channels were generated with cutoff radius 0.8, 1.0, and 1.0 a.u., respectively. Comparison of AE and pseudo wave functions shown in Fig. 1(a) is excellent. The agreement on the logarithmic derivatives is equally very good. An energy cutoff of 170 Ry is needed to achieve convergence in the atomic energy.

To calibrate the accuracy of the different Li pseudopotentials at very high pressure, the equation of states (EOS) of the $P4_132$ structure were calculated and compared with FP-LAPW calculations²¹ in Fig. 1(b). The $P4_132$ structure was chosen as the test case since it was suggested as the lowest enthalpy phase at high pressure, as well as the structural simplicity. The $P4_132$ is a cubic structure with the internal coordinates in $4a$ position, (3/8, 3/8, 3/8). All calculations were performed using a Monkhorst-Pack²² $16 \times 16 \times 16$ k -point mesh and Perdew-Burke-Ernzerhof (PBE) exchange-correlation functional.²³ The EOS calculated using pseudopotential plane-wave method with the TM and GTH pseudopotentials agree quantitatively with the FP-LAPW calculations over the entire pressure range. On the other hand, the EOS calculated using PAW pseudopotential agrees well with FP-LAPW results at low pressure but starts to deviate significantly at pressure higher than 200 GPa corresponding to Li electron-density $r_s < 1.94$. In terms of interatomic distance, the EOS starts to deviate when shortest Li-Li contact is smaller than 1.6 Å [see distance labels on

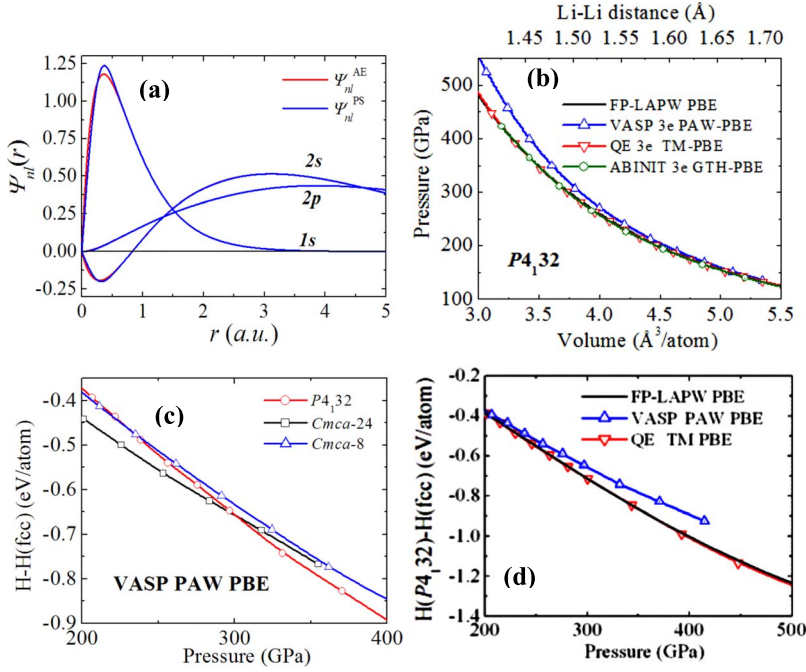


Fig. 1(b)]. This deviation indicates that the parameterizations of the Li PAW pseudopotential used in the present study might induce core overlap at high pressure. At 200 GPa, one half of the nearest-neighbor Li-Li distance from PAW calculation is 0.8 \AA , which is already shorter than the core cutoff radius of 0.82 \AA (or 1.55 a.u., see above). The calculated atomic volumes of $P4_132$ structure at selected pressures using different pseudopotentials are compared with the FP-LAPW results in Table I. For all pseudopotentials, the devia-

tion of calculated atomic volume from the FP-LAPW result becomes larger at greater pressure. The TM pseudopotential is the best choice with the smallest deviation, i.e., only 0.51% at 500 GPa. The GTH pseudopotential is also good, the deviation of which is about 1% at 500 GPa. The PAW pseudopotential works well up to 200 GPa with a reasonable deviation around 1%. However, at higher pressure, the deviation of PAW pseudopotential goes up quickly with pressure and exceeds 6% at 500 GPa. At very high pressure, a slight

FIG. 1. (Color online). (a) Comparison between the radial parts of the all-electron (AE) and pseudo (PS) wave functions in the hard TM pseudopotential generated for the QE package. (b) The EOS of the $P4_132$ structure calculated using FP-LAPW method and pseudopotential plane-wave method with different pseudopotentials. Top axis label: the closest Li-Li contact corresponding to the atomic volumes on the bottom axis. (c) Calculated enthalpies for the $P4_132$, $Cmca-8$, and $Cmca-24$ structures relative to the fcc structure using PAW pseudopotential. (d) Enthalpies of the $P4_132$ structure relative to the fcc structure calculated using FP-LAPW method and pseudopotential plane-wave method with different pseudopotentials.

TABLE I. The atomic volume of the $P4_132$ structure calculated using FP-LAPW method and pseudopotential plane-wave methods with three pseudopotentials at selected pressures. The number in the bracket after each atomic volume is the deviation from the FP-LAPW results. Structural parameters for the $P4_132$, $Cmca-8$, and $Cmca-24$ structures calculated using TM and TM pseudopotentials at 400 GPa.

Methods	V	V	V	V	V
	($\text{\AA}^3/\text{atom}$) at 100 GPa	($\text{\AA}^3/\text{atom}$) at 150 GPa	($\text{\AA}^3/\text{atom}$) at 200 GPa	($\text{\AA}^3/\text{atom}$) at 300 GPa	($\text{\AA}^3/\text{atom}$) at 500 GPa
FP-LAPW PBE	5.984(0.00%)	5.064(0.00%)	4.481(0.00%)	3.745(0.00%)	2.948(0.00%)
QE TM PBE	5.984(0.00%)	5.070(0.12%)	4.471(0.22%)	3.731(0.37%)	2.963(0.51%)
ABINIT GTH PBE	5.972(0.20%)	5.042(0.43%)	4.450(0.69%)	3.722(0.61%)	2.979(1.05%)
VASP PAW PBE	6.053(1.15%)	5.115(1.01%)	4.527(1.03%)	3.832(2.32%)	3.126(6.04%)

Structure	Pseudopotential	Lattice parameters	Atomic coordinates
		(\AA)	(fractional)
$P4_132$	VASP PAW PBE	$a=2.391$	$4a$ 0.3750 0.3750 0.3750
	QE TM PBE	$a=2.357$	$4a$ 0.3750 0.3750 0.3750
$Cmca-8$	VASP PAW PBE	$a=2.027$ $b=4.086$ $c=3.313$	$8f$ 0.5000 0.1389 0.4144
	QE TM PBE	$a=1.992$ $b=3.999$ $c=3.276$	$8f$ 0.5000 0.1331 0.4241
$Cmca-24$	VASP PAW PBE	$a=6.126$ $b=3.988$ $c=3.387$	$8f$ 0.0000 0.1534 0.0518 $16g$ 0.3343 0.1316 0.1087
	QE TM PBE	$a=5.999$ $b=3.623$ $c=3.644$	$8f$ 0.5000 0.1651 0.0584 $16g$ 0.3316 0.3915 0.1413

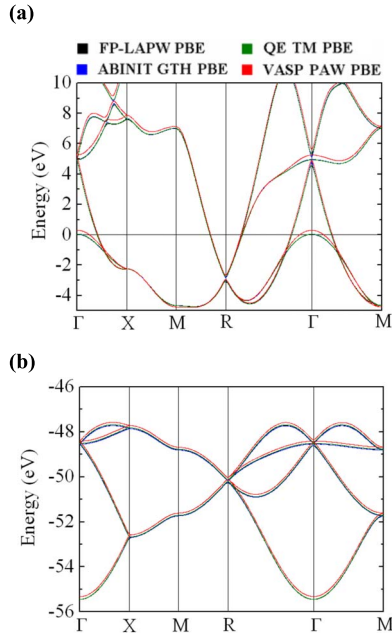


FIG. 2. (Color online). The calculated band structure of the $P4_132$ structure in the (a) valence and (b) core region using FP-LAPW method and pseudopotential plane-wave methods with different pseudopotentials. The corresponding Fermi level in each band structure is shifted to zero.

difference in atomic volume would induce significantly large error in calibrating the pressure. At 500 GPa, increasing the atomic volume of the $P4_132$ structure by 6% can offset the pressure by 80 GPa. At 1000 GPa, the error in calibrating the pressure using the PAW pseudopotential can be as high as 200 GPa. It should be noted that the lower accuracy of the Li PAW pseudopotential at high pressure or at high Li density is not a fundamental shortcoming of the PAW scheme, but the present results indicate a re-parameterization of the PAW pseudopotential (for Li) is needed in order to achieve the accuracy required for high-pressure applications. The structural parameters of three proposed high-pressure candidate structures of Li, $P4_132$, $Cmca-8$, and $Cmca-24$, calculated at 400 GPa using PAW and TM pseudopotentials are displayed in Table I. Similar to the $P4_132$ structure, the structural parameters of these structures calculated using PAW pseudopotential also show noticeable differences from the TM results. Same calculations have also been performed using the GTH pseudopotential, and the results are in quantitative agreement with the TM calculations.

To investigate the effect of core potential to the electronic structure, the valence and core electronic band structures of $P4_132$ structure computed using different pseudopotentials at same volume ($2.927 \text{ \AA}^3/\text{atom}$, close to 500 GPa) are compared with the FP-LAPW results in Figs. 2(a) and 2(b). The calculated dispersion of the valence and conduction bands with the TM and GTH pseudopotentials overlay on the FP-LAPW results. The gross band dispersion profiles from PAW calculations are consistent with the FP-LAPW results, but the details differ. For instance, the energy of the lowest energy doubly degenerated band crossing the Fermi surface at Γ is overestimated by the PAW calculation. The core orbital

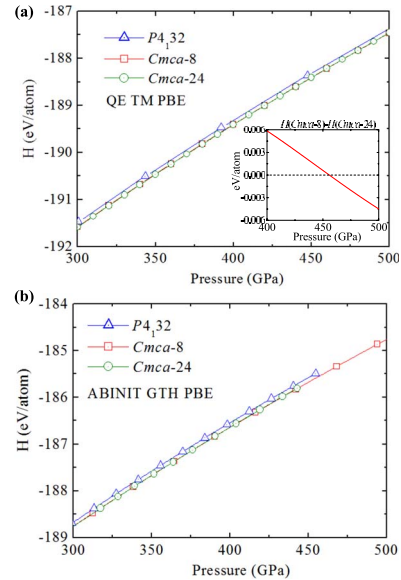


FIG. 3. (Color online) A comparison of the calculated enthalpies of $P4_132$ and $Cmca-8$ structures from 300 to 500 GPa using (a) TM and (b) GTH pseudopotentials. Inset: the enthalpy difference between $Cmca-8$ and $Cmca-24$ structures calculated using TM pseudopotential.

shows strong dispersion with the electron wave-vectors. The bandwidth of the $1s$ bands is 8 eV, almost double that of the valence bandwidth. All pseudopotentials nicely reproduced the FP-LAPW valence bandwidth. Again, the TM and GTH results are identical to the AE FP-LAPW calculations. Apart from a small shift to higher energy (0.1 eV), the PAW calculations are also very close to the FP-LAPW results. Analysis of the projected density of states (PDOS) shows strong mixing of valence $2p$ character in the core region, which results in the aspherically deformation of the core state. The integrated PDOS of the p orbital in the core region is $0.17e/\text{atom}$. The results show that the TM and GTH pseudopotentials can quantitatively reproduce the FP-LAPW results provided a converged plane-wave energy cutoff is used. While the PAW pseudopotential (with the default parameterizations) also gave band structure consistent with the FP-LAPW calculations [Fig. 2(a) and 2(b)], however, the calculated total energy at high pressure is not as accurate leading to serious errors in the EOS [Fig. 1(b)].

To investigate the reliability of the total energy calculated with the TM pseudopotential against the other pseudopotentials and FP-LAPW method the energetic order of $P4_132$, $Cmca-8$, and $Cmca-24$ structures is revisited. Using the PAW pseudopotential the same energetic order of the $Cmca-24$ and $P4_132$ structures as in a previous study⁸ is reproduced with $Cmca-24$ structure being the lowest enthalpy phase at pressure up to 300 GPa [Fig. 1(c)]. At higher pressure, the enthalpy of the $P4_132$ structure is lower than both $Cmca-24$ and $Cmca-8$ structures. In contrast, the stability order of $Cmca-8$ and $P4_132$ is reversed when the TM and GTH pseudopotentials [Figs. 3(a) and 3(b)] are used. Significantly, from 300 to 500 GPa, the same energy difference between $Cmca-8$ and $P4_132$ structures of *ca.* 0.1 eV is predicted by both pseudopotentials. Moreover, the $Cmca-24$

structure is found to be stable up to 456 GPa, at which pressure the *Cmca*-8 structure becomes more stable with a slightly lower enthalpy [inset of Fig. 3(a)]. The *P4*₁₃₂ structure, however, is not the lowest enthalpy phase up to at least 500 GPa, the highest pressure in the present study. To ensure the very small calculated energy difference is reliable and significant, the energy differences between *P4*₁₃₂ structure and a hypothetical fcc structure were computed using the TM pseudopotential, PAW pseudopotential, and FP-LAPW method. The enthalpy of *P4*₁₃₂ structure relative to fcc structure from 200 to 500 GPa is shown in Fig. 1(d). It is clear that the TM pseudopotential accurately reproduces both the trend and absolute energy difference as the FP-LAPW calculations. The weakness of the PAW pseudopotential in accurately reproducing the energetic at high pressure is again revealed by the large deviation from the FP-LAPW and TM results. The results clearly show the TM pseudopotential is highly reliable and the suggestion that *Cmca*-8 structure has a lower enthalpy than *Cmca*-24 structure above 456 GPa [Inset of Fig. 3(a)] is convincing. The *Cmca*-8 is the Li dimer structure proposed earlier.¹ It is shown here that it is indeed a competitive structure at higher pressure. From the analysis of the band structure,¹ it was suggested that *Cmca*-8 may undergo a Peierls distortion to an insulating lower symmetry structure.¹

In summary, it is found, as compared to FP-LAPW

method, the three-electron PAW Li potential supplied with the VASP pseudopotential library is able to provide reliable physical quantities at pressures lower than 200 GPa, or when $r_s > 1.94$ and Li-Li distance is larger than 1.6 Å. However, at greater pressure, the PAW results start to deviate more significantly from the FP-LAPW results. Therefore, caution must be taken in using this potential to examine small energetic differences between competitive polymorphs⁸ of Li and in the study of the structure and dynamics of the liquid⁹ at very high pressure. A re-parameterization of the PAW pseudopotential using tighter criteria for the core states can certainly improve the transferability and the reliability at high pressure. On the other hand, the GTH pseudopotential used in conjunction with the ABINIT code is reliable over a large pressure range. The TM pseudopotential developed here and intended to be used with the QE package performs as well. It is shown the “dimer” *Cmca*-8 structure is slightly energetically more favorable than the previously proposed *Cmca*-24 structure above 456 GPa. The recently proposed *P4*₁₃₂ structure is not energetically favorable up to at least 500 GPa.

ACKNOWLEDGMENT

Y.Y. gratefully acknowledges Axel Kohlmeyer for helpful suggestions on the construction of the Li pseudopotential.

¹J. B. Neaton and N. W. Ashcroft, *Nature (London)* **400**, 141 (1999).

²R. Rousseau, K. Uehara, D. D. Klug, and J. S. Tse, *ChemPhysChem* **6**, 1703 (2005).

³D. M. Deaven and K. M. Ho, *Phys. Rev. Lett.* **75**, 288 (1995).

⁴A. R. Oganov and C. W. Glass, *J. Chem. Phys.* **124**, 244704 (2006).

⁵G. Trimarchi and A. Zunger, *Phys. Rev. B* **75**, 104113 (2007).

⁶N. L. Abraham and M. I. J. Probert, *Phys. Rev. B* **73**, 224104 (2006).

⁷G. Kresse and D. Joubert, *Phys. Rev. B* **59**, 1758 (1999).

⁸Y. Ma, A. R. Oganov, and Y. Xie, *Phys. Rev. B* **78**, 014102 (2008).

⁹I. Tamblyn, J.-Y. Raty, and S. A. Bonev, *Phys. Rev. Lett.* **101**, 075703 (2008).

¹⁰S. A. Bonev, E. Schwegler, T. Ogitsu, and G. Galli, *Nature (London)* **431**, 669 (2004).

¹¹At ambient pressure, the electron-binding energy for Li 1s orbital is 54.7 eV (Ref. 12). Since the Fermi energy of Li is around 4.7 eV (Ref. 13), a rough estimate of the core-valence separation is 50.0 eV.

¹²J. K. Kirz, D. T. Attwood, M. R. Howells, K. D. Kennedy, K.-J. Kim, J. B. Kortright, R. C. Perera, P. Pianetta, J. C. Riodan, J. H. Scofield, G. L. Stradling, A. C. Thompson, J. H. Underwood, D. Vaughn, G. P. Williams, and H. Winick, *X-ray Data Booklet* (Center for X-ray Optics, Lawrence Berkeley Laboratory, Berkeley, 2001), <http://xdb.lbl.gov>

¹³N. W. Ashcroft and N. D. Mermin, *Solid State Physics* (Saunders, Philadelphia, 1976).

¹⁴M. Krack, *Theor. Chem. Acc.* **114**, 145 (2005).

¹⁵G. Kresse and J. Furthmüller, *Comput. Mater. Sci.* **6**, 15 (1996).

¹⁶X. Gonze, J.-M. Beuken, R. Caracas, F. Detraux, M. Fuchs, G.-M. Rignanese, L. Sindic, M. Verstraete, G. Zerath, F. Jollet, M. Torrent, A. Roy, M. Mikami, Ph. Ghosez, J.-Y. Raty, and D. C. Allan, *Comput. Mater. Sci.* **25**, 478 (2002); X. Gonze, Z. Kristallogr. **220**, 558 (2005), see also <http://www.abinit.org>

¹⁷J. K. Dewhurst, S. Sharma, and C. G. Ambrosch-Draxl, the EXCITING FP-LAPW code (<http://exciting.sourceforge.net/>).

¹⁸P. Blaha, K. Schwarz, G. K. H. Madsen, D. Kvasnicka, and J. Luitz, *WIEN2K, An Augmented Plane Wave Plus Local Orbitals Program for Calculating Crystal Properties* (Karlheinz Schwarz, Technische Universität Wien, Austria, 2002).

¹⁹N. Troullier and J. L. Martins, *Phys. Rev. B* **43**, 1993 (1991).

²⁰QUANTUM-ESPRESSO is a community project for high-quality quantum-simulation software, based on density-functional theory, and coordinated by Paolo Giannozzi. See <http://www.quantum-espresso.org> and <http://www.pwscf.org>

²¹Since both the all-electron full potential linearized plane-wave codes EXCITING and WIEN2K produced almost identical results, therefore, only the results obtained from EXCITING are reported here. In the AE FP-LAPW calculations, since the size of a Li atom is very small, a small muffin-tin radius ($RK_{\max}=10$) together with a large plane-wave expansion ($l_{\max}=12$) must be used in order to achieve converged results.

²²H. J. Monkhorst and J. D. Pack, *Phys. Rev. B* **13**, 5188 (1976).

²³J. P. Perdew, K. Burke, and M. Ernzerhof, *Phys. Rev. Lett.* **77**, 3865 (1996).